Journal of Drug Delivery Science and Technology 120 (2026) 108278

Contents lists available at ScienceDirect

Journal of Drug Delivery Science and Technology

journal homepage: www.elsevier.com/locate/jddst

3D-printed detachable tablets for flexible dosing in personalized medicine: Influence of score geometry and printing technology

Gabriel S. Oliveira [a], Ana Luiza Lima [a], Idejan P. Gross [a], Ludmila Alvim Gomes Pinho [a], Livia Sa-Barreto [b], Patrícia Medeiros-Souza [c], Tais Gratieri [a], Guilherme M. Gelfuso [a], Marcilio Cunha-Filho [a,*]

[a] Laboratory of Food, Drugs, and Cosmetics (LTMAC), University of Brasilia, Brasilia, DF, 70910-900, Brazil
[b] Faculty of Ceilandia, University of Brasilia (UnB), Brasília, DF, 72220-900, Brazil
[c] School of Health Sciences, University of Brasilia (UnB), Brasília, DF, 72220-900, Brazil

ARTICLE INFO

Keywords:
3D-printing
Personalized medicine
Fused deposition modeling
Binder jetting
Detachable tablet

ABSTRACT

Tablet subdivision is widely used for dosage adjustment, particularly in pediatrics and geriatrics, but conventional splitting often leads to poor dose uniformity, increased friability, and stability issues. This study explored the feasibility of two leading 3D printing technologies, fused deposition modeling (FDM) and binder jetting (BJ), for producing detachable tablets specifically designed for accurate subdivision. Tablets were designed with distinct score geometries (continuous and dotted) and fabricated using PVA (FDM) or calcium sulfate (BJ). In addition, a representative drug-loaded FDM sample was also evaluated. BJ tablets were further treated with saline to enhance structural cohesion. The printed dosage forms were systematically characterized for mass variation, mass loss, friability, pore volume, and morphology. Results demonstrated that FDM tablets achieved the highest performance, with mass variation consistently below 2% and negligible mass loss (<0.1%), even after subdivision into eighths, with comparable subdivision accuracy observed for the drug-loaded formulation. BJ tablets showed greater variability but achieved acceptable results when optimized with dotted-score design and saline post-treatment, with friability values (~0.3%), well below the 1% pharmacopeial limit. Morphological analyses confirmed improved cohesion and reduced porosity after post-treatment. Overall, these findings demonstrate the potential of 3D printing to overcome the limitations of conventional tablet splitting by enabling dosage forms specifically engineered for accurate and reproducible subdivision. This approach may complement both individualized and large-scale pharmaceutical manufacturing scenarios.

1. Introduction

Tablet subdivision into two or more parts is a common practice among patients and healthcare professionals, mainly to adjust dosage, facilitate swallowing, or reduce therapeutic costs [1–3]. However, this practice involves several risks, including compromised product stability, unintended operator exposure, and, most critically, dosage variability. Such variability can compromise therapeutic efficacy and potentially introduce toxicity risks [4–6]. Vulnerable populations, such as pediatric and elderly patients, are especially affected [7]. In fact, in pediatric populations, subdivision is often required due to the limited availability of age-appropriate dosage strengths and the need for weight-based dosing. In geriatric patients, subdivision becomes equally critical to enable individualized therapy in the context of comorbidities, age-related renal/hepatic decline, polypharmacy, and dysphagia [8,9].

The current powder compaction technology used in industrial manufacturing has inherent limitations in ensuring uniform fragments. Indeed, compacted matrices exhibit microstructural features that are challenging to control during compression, leading to unpredictable splitting outcomes [10,11]. As a result, uniform dosing across subdivided units cannot be guaranteed [12–14], evidencing the need for alternative manufacturing technologies capable of producing tablets that can be safely and reliably divided [15].

Despite the pharmaceutical industry's challenges in manufacturing subdivisible tablets with assured quality, the demand for personalized pharmacotherapy has never been greater. Contemporary therapeutic approaches increasingly emphasize individualized treatment, tailored to patient-specific characteristics such as age, disease stage, genetic profile,

* Corresponding author.
E-mail address: marciliofarm@hotmail.com (M. Cunha-Filho).

https://doi.org/10.1016/j.jddst.2026.108278
Received 28 October 2025; Received in revised form 14 March 2026; Accepted 25 March 2026
Available online 25 March 2026

and comorbidities [16]. In practice, off-label tablet splitting is becoming more frequent, often relying on imprecise methods such as kitchen knives or scissors, underscoring the urgent need for more reliable technological solutions [17–19]. Critical examples include pediatric antiepileptics such as phenytoin and phenobarbital, and the high-potency antipsychotic haloperidol, widely prescribed in geriatrics. In such cases, dosing frequently requires splitting tablets into four or more fragments, rendering the final dose unpredictable and the subdivision procedure inherently risky [20,21].

Currently, three-dimensional (3D) printing technologies have gained significant traction in drug delivery, emerging as promising tools for the manufacture of personalized and innovative dosage forms. These technologies combine electronic precision, modulation of drug release profiles, and adaptability to individual patient needs [22,23]. Among the many 3D printing techniques, two have attracted particular attention in the pharmaceutical arena: Fused Deposition Modeling (FDM) and Binder Jetting (BJ). FDM stands out for its relatively low cost, reproducible control of printed structures, and applicability at both laboratory and industrial scales [24–26]. In contrast, BJ offers unique advantages such as room-temperature processing, enhanced porosity of the printed structures, and feasibility for large-scale production [27,28]. Both technologies directly address the clinical demand for treatment customization, enabling the incorporation of multiple drugs and tailored release profiles within a single dosage unit. Such drug combination in a single formulation is particularly relevant for the elderly population, who are often subject to polypharmacy [29].

Nevertheless, the current clinical landscape increasingly demands not only dose personalization but also practical flexibility for dose adjustment during treatment. In many clinical settings, dose titration must be implemented rapidly in response to dynamic physiological or therapeutic variables, sometimes within the interval between consecutive doses. Such situations are common in patients undergoing chemotherapy, immunosuppressed transplant recipients, and individuals with diabetes, where treatment regimens are frequently adjusted according to laboratory results or clinical monitoring. Although 3D printing enables the production of individualized dosage units, generating a new tablet for each dose adjustment may not always be feasible in routine practice. In these scenarios, dosage forms specifically engineered to allow accurate and reproducible tablet subdivision can provide an additional and practical layer of therapeutic flexibility.

Traditional pharmaceutical manufacturing relies on compression of powder blends, and fracture propagation during tablet splitting is largely uncontrolled, often resulting in substantial dose variability. In contrast, additive manufacturing can enable the rational design of fracture-guiding geometries, allowing the subdivision process to be engineered during the design stage. This capability opens new opportunities to improve dose accuracy and reproducibility during tablet subdivision, particularly for populations in which dose splitting is frequently required, such as pediatric and geriatric patients.

Furthermore, while 3D printing is often associated with fully individualized production, some additive manufacturing technologies, particularly binder jetting (BJ), also show strong potential for semi-industrial or industrial-scale pharmaceutical manufacturing. In such scenarios, dose personalization may still be constrained by the production of fixed nominal strengths, similarly to conventional pharmaceutical manufacturing. Indeed, the first FDA-approved 3D-printed medicine, Spritam® (levetiracetam), produced using BJ technology, is manufactured industrially in predefined strengths [25]. Under these conditions, detachable tablets may expand dose flexibility within a limited set of manufactured strengths, reducing the need for multiple product variants while still enabling individualized dose adjustments at the point of use.

For these reasons, detachable tablets should not be viewed as an alternative to individualized 3D printing, but rather as a complementary strategy that may enhance the practical applicability of additive manufacturing across both point-of-care and large-scale pharmaceutical production settings.

Therefore, this study investigates the feasibility of designing detachable tablets using two widely explored pharmaceutical 3D printing technologies, fused deposition modeling (FDM) and BJ, for producing safer, more reliable, subdivisible tablets. To this end, detachable-scored tablets were designed for each technology and specifically adapted to allow accurate manual subdivision into multiple parts. For this exploratory study, matrices commonly used for each technique were selected, namely polyvinyl alcohol (PVA) for FDM and calcium sulfate hemihydrate for BJ [27]. In addition, to enhance the translational relevance of the study, a representative drug-loaded FDM filament formulation was also evaluated. The printed dosage forms were characterized in terms of mechanical properties, morphology, and microstructure to demonstrate their potential for precise and reproducible dose subdivision.

2. Materials and methods

2.1. Materials

VisiJet PXL Core (calcium sulfate hemihydrate), VisiJet PXL Clear binder, and Ware Cure Solution (magnesium sulfate heptahydrate) were obtained from 3D Systems (Rock Hill, SC, USA). Parteck® MXP (PVA, polyvinyl alcohol, lot F2304664422) was acquired from Merck KGaA (Darmstadt, Hesse, Germany). Caffeine (lot BCBS9512V) was purchased from Sigma-Aldrich (St. Louis, MO, USA). Glycerol (lot 129,208) was obtained from Dinâmica (São Paulo, Brazil).

2.2. 3D models of detachable tablets

The detachable tablet models were designed using Tinkercad software [30,31]. The initial design consisted of a flat circular tablet, a geometry commonly employed in industrial tablet manufacturing, with a diameter of 15 mm and a height of 6 mm. Based on this template, different score configurations were implemented to enable subdivision into halves, quarters, and eighths, without the need for auxiliary tools such as tablet splitters or knives (Fig. 1). After tests with the two selected 3D printing techniques, three final models were selected for this study.

The tablets produced by BJ were designed to contain score lines in two distinct geometric configurations. The first configuration consisted of a continuous score line with a width of 1 mm and a depth of 2.5 mm. The second configuration featured a dotted score line composed of discontinuous 2 mm segments distributed along the scoring path. Both models had identical external dimensions (15 mm in diameter and 6 mm in height) differing only in the internal geometry of the score line, as illustrated in Fig. 2. In contrast, for the FDM model, a more pronounced central score was required to allow manual subdivision. This modification consisted of a deeper (5 mm) and wider (1 mm) slit, resulting in a more prominent separation of the planned fractions (Fig. 2). Such an adaptation was necessary to compensate for the greater hardness and elasticity of the thermoplastic matrix used in the FDM platform.

For FDM printing, a Creality CR-10 SE 3D printer (Shenzhen, China) was employed. Previously, a drug-loaded filament was produced based on PVA plasticized with glycerol (8%, w/w) and containing caffeine as a model API (20%, w/w), adapted from a previously reported formulation [32]. The filament was prepared by hot-melt extrusion without recirculation using a co-rotating conical twin-screw extruder (HAAKE MiniCTW, ThermoScientific, Waltham, MA, USA) operated at 160 °C and 50 rpm with a die diameter of 1.8 mm. The extruder was coupled to a filament tractor equipped with an air-cooling system and an automated diameter measurement device (FTR1, Filmaq3D, Curitiba, Brazil). A placebo formulation containing PVA (90%, w/w) and glycerol (10%, w/w) was also produced under the same processing conditions.

The obtained filaments were printed under the following conditions: nozzle temperature 180 °C, bed temperature 50 °C, nozzle diameter 0.4 mm, layer height 0.2 mm, and printing speed 20 mm/s, using a

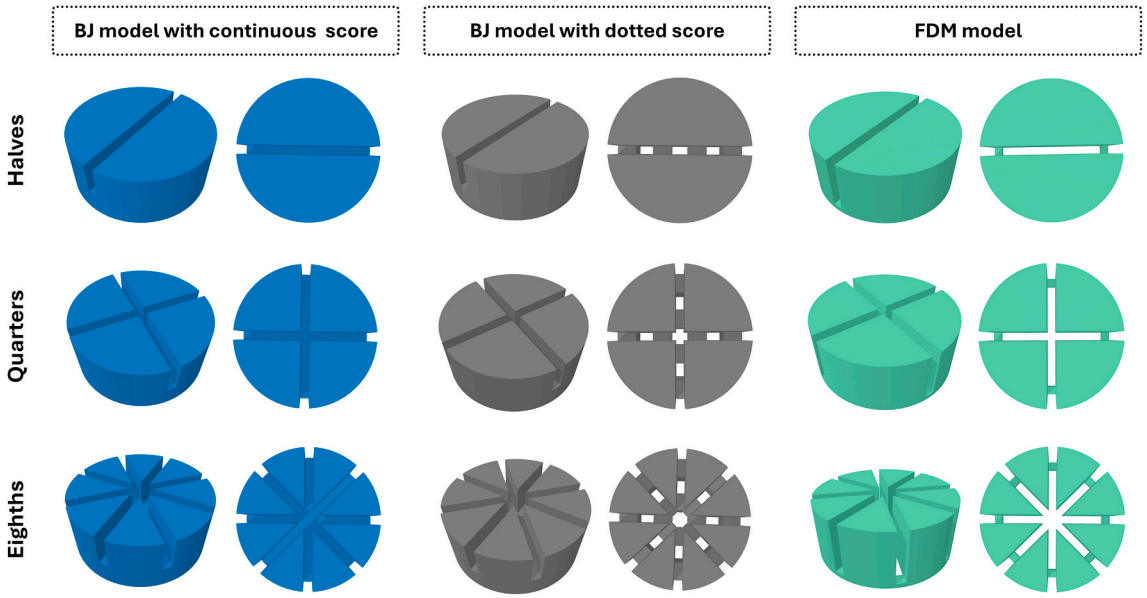

Fig. 1. 3D tablet models designed for subdivision into halves, quarters, and eighths, using binder jetting (BJ) and fused deposition modeling (FDM).

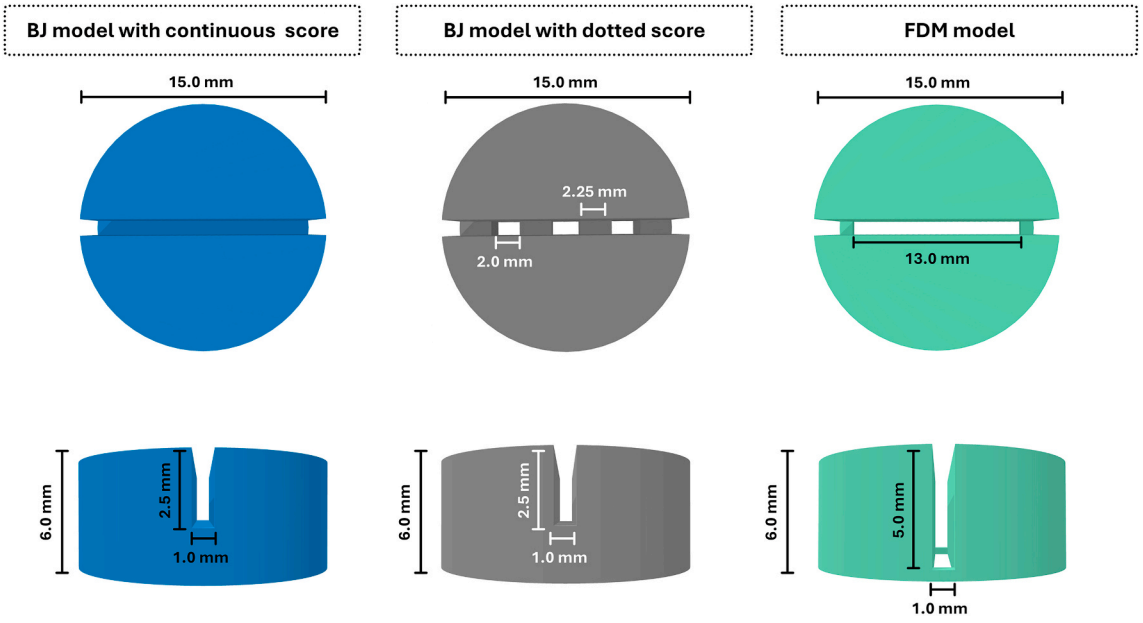

Fig. 2. 3D models of detachable tablets designed for binder jetting (BJ) and fused deposition modeling (FDM), showing score lines configurations. Cross-sectional views illustrate the depth, width, and structural design of the score lines required to optimize fracture propagation.

zigzag infill pattern. An infill density of 20% was selected based on preliminary trials indicating that this condition provides adequate mechanical cohesion while still allowing controlled fracture propagation during tablet subdivision. This infill level was therefore adopted as a representative operational printing condition for the study.

For BJ, tablets were fabricated on a ProJet® 460Plus 3D printer (3D Systems, Rock Hill, SC, USA), using VisiJet PXL Core (calcium sulfate hemihydrate) as the powder base and VisiJet PXL Clear as the binder. Key parameters included a layer thickness of 0.1 mm and a print head resolution of 300 × 450 dpi (x, y). Following printing, tablets were carefully removed from the powder bed and subjected to depowdering using compressed air.

2.3. Post-treatment of binder jetting tablets

The need for post-treatment of tablets produced by BJ was preliminarily assessed using different subdivision designs and treatment conditions. Three tablet geometries (subdivision into 2, 4, and 8 parts) and three post-treatment conditions were evaluated: (i) no solution applied; (ii) application of 200 μL (100 μL per face); and (iii) application of 400 μL of saline solution (200 μL per face). The solution, supplied by the printer manufacturer, consisted of Epsom salt (magnesium sulfate heptahydrate) in water, intended to enhance surface hardness and cohesion of the printed structures. The application was performed using a volumetric pipette via controlled dropwise addition to ensure precise volume deposition on each tablet. After treatment, the tablets were allowed to dry at room temperature (around 25 °C) for at least 24 h to ensure complete solvent evaporation and structural stabilization. Tablets were

manually subdivided, and mass loss was determined as described in the subsequent section.

Morphological analysis of BJ tablet surfaces was performed using scanning electron microscopy (SEM; JEOL JSM-7001F, Tokyo, Japan). Before analysis, samples were sputter-coated with a thin metallic layer to ensure conductivity and suitability for high-vacuum observation. This assay aimed to evaluate the surface microstructure of tablets, enabling visualization of particle distribution, pore presence, and matrix compactness.

2.4. Mass measurements

3D-printed detachable tablets were manually subdivided into halves, quarters, or eighths according to the pre-designed scores. Each tablet was weighed on an analytical balance (AUY 220, Shimadzu, Kyoto, Japan) before and after subdivision (n = 10). The percentage mass variation was calculated as the deviation between the measured mass of each subdivided fraction (Md) and the theoretical mass, obtained by dividing the intact tablet mass (Mw) by the number of subdivisions (Q), as shown in Equation (1).

$$Mass\ variation\ (\%) = \left| 100 - \left(\frac{100 \times Md}{Mw/Q} \right) \right| \quad \text{(Equation 1)}$$

The mass loss originating from fragmenting and/or powdering was expressed as a percentage and calculated from the difference between the initial mass (Mw) of the whole tablet and the sum of the respective tablet fraction's mass, as indicated in Equation (2).

$$Mass\ loss\ (\%) = \left[\frac{\left(Mw - \sum_{i=o}^{\infty} Md \right) \times 100}{Mw} \right] \quad \text{(Equation 2)}$$

Statistical analyses were performed using Jamovi software (version 2.6). Data were first evaluated for normality and homoscedasticity. The Kruskal–Wallis test was applied to detect overall differences among the groups, followed by the Dwass–Steel–Critchlow–Fligner post hoc test for multiple pairwise comparisons. Statistical significance was established at $p < 0.05$.

2.5. Friability

The friability test was performed in accordance with USP guidelines [33] using a SP Labor friabilator (model SP-FR, N°S:00119/008, São Paulo, Brazil) to evaluate the tablets' abrasion resistance. Samples were weighed, placed in the friabilator drum, and subjected to 100 rotations at 25 ± 1 rpm.

Twenty fragments of whole, halved, quartered, or eighth tablets were weighed before (Wb) and after (Wa) the friability test. Tablets with an individual mass ≥650 mg were used, in accordance with pharmacopeial recommendations for friability testing [33]. Any adhering powder was carefully removed from the tablet surfaces to prevent fine particles from interfering with the measurement. Friability was then calculated according to Equation (3):

$$Friability\ (\%) = \frac{(Wb - Wa) \times 100}{Wb} \quad \text{(Equation 3)}$$

2.6. Determination of porosity

The porosity of the tablets was determined to estimate the fraction of the internal structure occupied by pores. For this purpose, a combined approach using three-dimensional modeling and gas pycnometry was employed.

The total apparent volume (Vi) of each tablet was obtained from the. stl file generated during the three-dimensional modeling process using Meshmixer software (Autodesk, version 3.5.474). This software calculates the solid's geometric volume from its three-dimensional mesh. The effective volume (Vf) was determined by gas pycnometry using an Ultrapyc 5000 Micro instrument (Anton Paar, Ashland, VA, USA) with ultra-high purity nitrogen as the displacement gas. This technique enables the measurement of the true volume occupied by the solid material, excluding the void spaces accessible to the gas.

The porosity (VP%) was calculated from the difference between the total and effective volumes according to Equation (4):

$$Porosity\ (\%) = \frac{(Vi - Vf) \times 100}{Vi} \quad \text{(Equation 4)}$$

ANOVA was performed, followed by Tukey's post hoc test for pairwise comparisons. Statistical significance was established at $p < 0.05$.

2.7. Optical microscopy

Whole and subdivided 3D tablets were examined using a stereomicroscope (SZT model, Laborana, São Paulo, Brazil) at a 2 × magnification. The images obtained enabled the identification of structural defects, such as microcracks, chipping, and particle detachment, as well as the assessment of the integrity of the pre-designed score regions. This analysis provided complementary morphological evidence regarding the quality of the fracture surfaces and the efficiency of the subdivision design.

3. Results and discussion

3.1. Post-treatment of BJ tablets

Post-processing is a commonly required step in BJ 3D printing, aimed at enhancing the mechanical strength and structural cohesion of the printed object [27]. In the specific context of tablet subdivision, one of the approaches evaluated in this study was the application of a magnesium sulfate (Ware Cure Solution) solution.

Mass loss testing was employed to assess the effectiveness of the post-treatment in maintaining the integrity of BJ-printed tablets. The results demonstrated that solution application significantly reduced material loss upon subdivision, indicating improved cohesion and mechanical robustness of the subdivided tablets (Table 1). This effect was particularly relevant in tablets with more complex subdivision geometries, which exhibited greater structural fragility in the absence of treatment.

Among the evaluated conditions, the 400 μL application volume yielded the most favorable outcomes, with minimal mass loss across all tested geometries. These findings suggest that this level of post-treatment promotes surface consolidation of the tablets, thereby improving their stability during handling and subdivision.

SEM analysis revealed marked morphological differences between tablets with and without post-treatment using the saline solution. In the untreated samples, the micrographs showed a highly porous and disorganized surface, characterized by poorly compacted particles and loosely connected interparticulate voids (Fig. 3). This morphology highlights the weak cohesion among matrix constituents, which likely explains the higher mass loss observed in the preliminary subdivision

Table 1
Mass loss after subdivision of binder jetting tablets with and without saline post-treatment.

Number of subdivisions	Mass loss (%)		
	No post-treatment	Post-treatment 200 μL	Post-treatment 400 μL
Halves	0.14 ± 0.07^{a}	0.08 ± 0.03^{d}	0.02 ± 0.01^{e}
Quarters	0.44 ± 0.07^{b}	0.14 ± 0.03^{a}	0.05 ± 0.01^{e}
Eighths	1.26 ± 0.52^{c}	0.59 ± 0.25^{b}	0.13 ± 0.03^{a}

Different superscript letters (a–e) indicate statistically significant differences ($p < 0.05$) according to Dwass–Steel–Critchlow–Fligner.

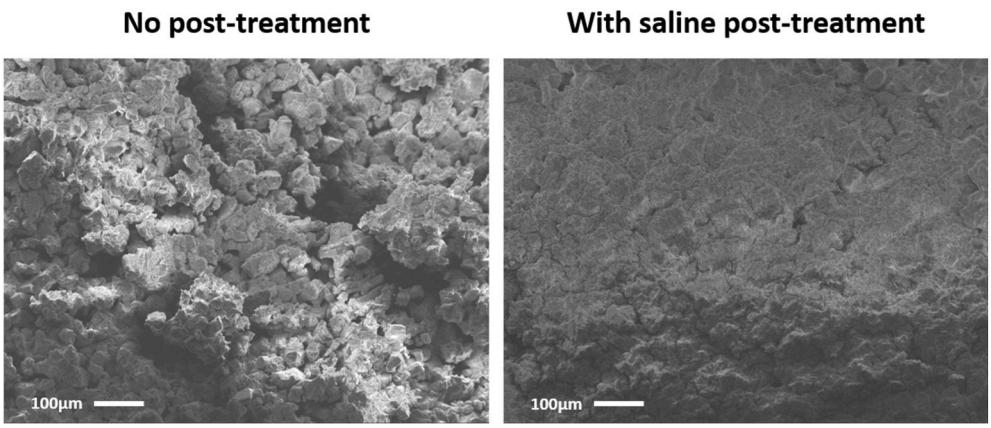

Fig. 3. Scanning electron microscopy images of tablets with and without saline post-treatment (400 µL), at magnifications of 120 × .

tests, particularly in tablets designed with multiple score lines.

In contrast, the tablets subjected to post-treatment with saline exhibited a visibly denser, more compact microstructure. The particles showed improved interconnection, with partial filling of superficial pores and a more uniform organization, indicating that the solution effectively acted as a surface-binding agent. This enhancement in matrix cohesion facilitated the subdivision process. Indeed, significantly lower mass loss values were recorded for the post-treated tablets, particularly under the 400 µL condition, which consistently yielded the smallest variation after splitting.

These findings are consistent with previous studies demonstrating that saline post-treatment enhances interparticulate bonding by promoting the formation of solid bridges through a mechanism commonly referred to as cold recrystallization sintering [27,34]. In this process, the applied liquid solution acts as a temporary vehicle, partially dissolving surface regions of the solid particles and enabling their reorganization, followed by recrystallization that generates stronger and more cohesive bonds between the particulate components. Such a consolidation mechanism explains the improved structural integrity and reduced mass loss observed in the treated tablets. Based on these results, all subsequent experiments in this study were conducted exclusively with tablets subjected to post-treatment with 400 µL of saline solution per unit.

3.2. Mass measurements

One of the most critical requirements in tablet subdivision is the ability to generate fragments of equivalent mass, which, in the case of homogeneous solid matrices, should correspond to equal drug dosage [3,35]. In conventional commercial tablets, recent studies have reported that mass variation after subdivision into halves may reach up to 50% of the intended dose [3]. In contrast, quartering can lead to alarming deviations of up to 60% from the target mass [35]. Subdivision into eighths is not feasible with traditional manufacturing technologies, and no reliable source data are available; however, off-label medical practice reports instances of multiple tablet fragmentations [1]. For instance, in pediatric onco-hematology, chemotherapeutic tablets such as mercaptopurine are frequently split—sometimes into as many as one-eighth of a tablet—thereby increasing the risk of dose inaccuracy at an unacceptable level [36].

The 3D-printed detachable tablets demonstrated clear superiority over the subdivision of conventional commercial tablets (Fig. 4). For halves, the mean mass variation observed with 3D printing was below 1.5%, representing a nearly 7-fold reduction compared to the typical variability reported for market tablets [3]. Similarly, detachable tablets subdivided into quarters also performed remarkably well, with mass variation not exceeding 4%. Subdivision into eighths, which is generally considered impractical using conventional manufacturing, yielded highly promising results with 3D printing: FDM drug-loaded and placebo tablets exhibited mean mass variations of 1.4 ± 1.1% and 1.5 ± 1.3%, respectively, whereas BJ dotted-score tablets showed a higher variation of 3.8 ± 3.1%. Nevertheless, all values remained well within the FDA acceptance limit of ±10% for split tablets [37].

When comparing the two 3D printing platforms, FDM consistently produced lower mass variation values, which can be attributed to the plastic and cohesive nature of PVA matrices. Notably, the incorporation of the drug into the PVA polymeric matrix did not affect subdivision performance, as no statistically significant differences were observed compared with placebo FDM tablets. A previous study from our group further corroborates this finding, showing that polymer-based matrices exhibit a more uniform and mechanically robust internal structure, thereby improving their suitability for subdivision. In that work, Soluplus-based tablets displayed a mean mass variation of 3.9% for halves [38].

The introduction of the dotted-score design in BJ tablets reduced mass variation, particularly in more complex subdivisions (quarters and eighths). In contrast, FDM tablets consistently maintained low variability under all conditions, reaching only 1.72 ± 2.35% in the eighths, further reinforcing their excellent performance in multiple subdivisions. Importantly, similar subdivision accuracy was observed for tablets printed from the drug-loaded filament, despite the known influence of drug incorporation on the rheological and mechanical behavior of FDM matrices. In this case, the mean mass variation remained below 1.5% across halves, quarters, and eighths, matching that of the placebo FDM tablets. From a clinical perspective, these values represent a substantial improvement over conventional commercial tablets.

In conventional commercial tablets, subdivision commonly leads to crumbling at the fracture site, resulting in unintended dose loss. Regulatory standards stipulate that such loss should not exceed 3% [37]. However, studies have shown that splitting conventional tablets often results in a significant reduction in mechanical strength, leading to mass losses exceeding 10% [3,35]. In this respect, the detachable 3D-printed tablets achieved particularly impressive results (Fig. 5). Even when subdivided into eighths, mass loss remained below 0.3%. Once again, FDM (placebo or drug-loaded) emerged as the standout technology, showing nearly negligible mass loss, underscoring its robustness and suitability for accurate subdivision. Regarding the BJ models, the dotted-score design again demonstrated superior performance compared to the continuous-score, regardless of the subdivision level. This finding highlights that score geometry plays a decisive role in determining the mechanical strength, fracture propagation, and structural integrity of the printed tablets.

3.3. Friability

The friability of subdivided tablets is a critical quality attribute, since the resulting fractions are typically handled by patients and stored for

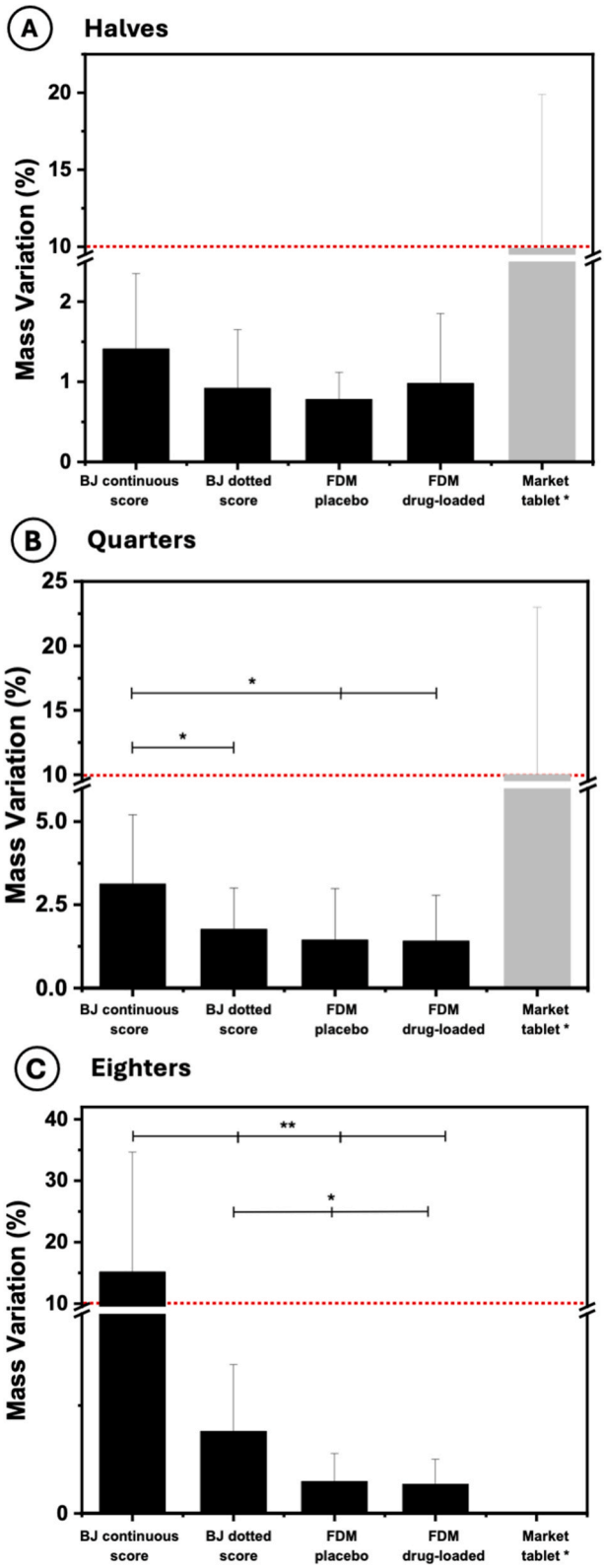

Fig. 4. Mass variation (%) of detachable 3D-printed tablets fabricated by binder jetting (BJ)—with continuous or dotted score designs—and fused deposition modeling (FDM) —placebo or drug-loaded. Tablets were manually divided into (A) halves, (B) quarters, and (C) eighths. Comparative data for commercial tablets were obtained from the literature ($^{\#}$ [3]; $^{\#\#}$ [35]). ϕ = no data available. The dashed line indicates the FDA's guidelines for tablet splitting. * ($p < 0.05$), ** ($p < 0.005$).

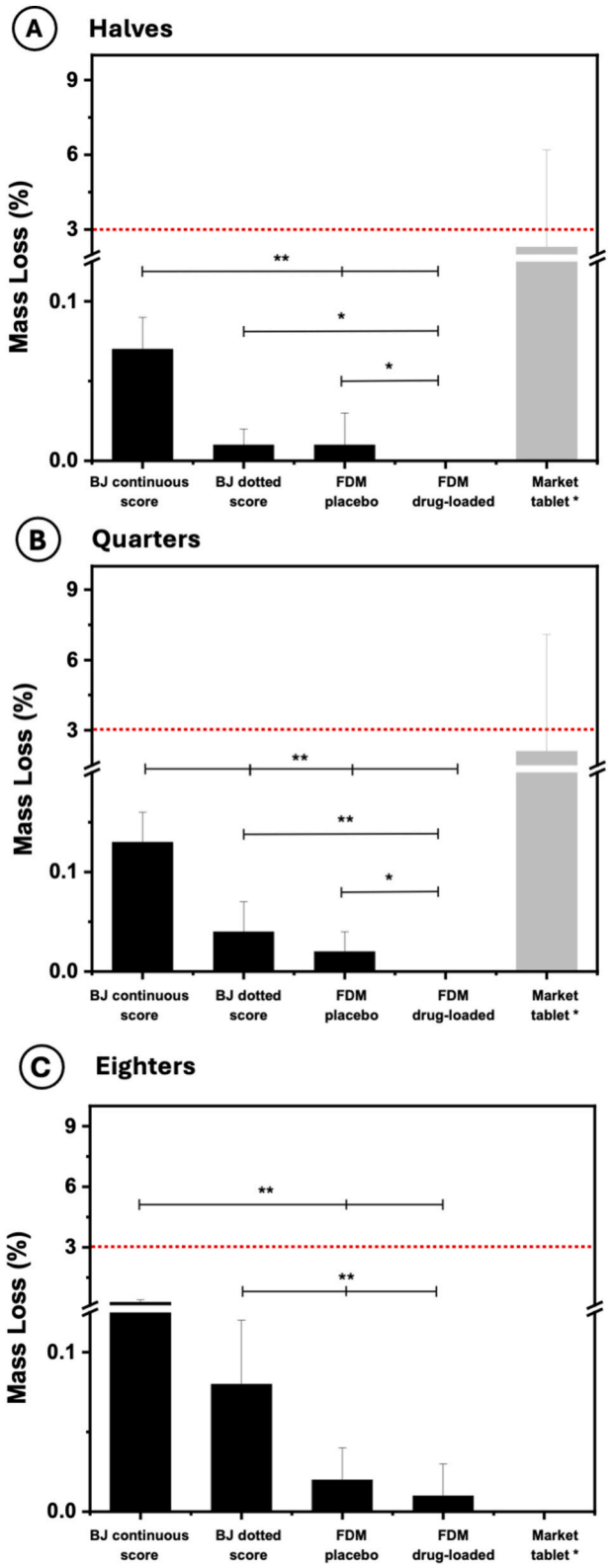

Fig. 5. Mass loss (%) of detachable 3D-printed tablets fabricated by binder jetting (BJ)—with continuous or dotted score designs—and fused deposition modeling (FDM) —placebo or drug-loaded. Tablets were manually divided into (A) halves, (B) quarters, and (C) eighths. Comparative data for commercial tablets were obtained from the literature ($^{\#}$ [3]; $^{\#\#}$ [35]). ϕ = no data available. The dashed line indicates the FDA's guidelines for tablet splitting. * ($p < 0.05$), ** ($p < 0.005$).

subsequent use – conditions that can lead to additional mass loss and, consequently, unintended dose reduction [11].

In this study, all friability values remained well below the pharmacopoeial limit of 1% (Fig. 6). Particularly, the plastic matrices of FDM-printed detachable tablets demonstrated exceptional mechanical robustness, with negligible friability values across all subdivisions. Once again, the incorporation of the model drug into the polymeric matrix, even at a relatively high loading of 20% (w/w), did not compromise the mechanical properties of the FDM detachable tablets. This observation is consistent with previous reports on polymeric tablets composed of continuous matrices, which are sufficiently rigid to withstand impact stresses and thereby minimize material loss by chipping or crushing [38].

In contrast, powder-based matrices, such as those produced by BJ, often pose greater challenges in terms of mechanical performance. Conventional subdivision of powder-compacted tablets usually results in friability values exceeding pharmacopoeial specifications (Fig. 6). Indeed, a recent study reported friability levels above 1.5% for halved and quartered tablets, mainly due to fragile edges and reduced mechanical strength after fracture [35]. Against this background, the friability outcomes achieved with BJ 3D-printed detachable tablets in the present work are particularly remarkable, with values of approximately 0.3%, below the 1% pharmacopoeial threshold.

The enhanced performance of BJ tablets can be attributed to the saline post-treatment, which played a decisive role in strengthening the particulate matrix. As evidenced by SEM analysis, the application of a magnesium sulfate solution led to partial filling of surface pores, improved particle interconnection, and greater uniformity of the matrix microstructure [27,34]. These newly formed bonds markedly increased matrix cohesion, thereby reducing friability and improving the tablets' resistance to handling and storage stresses.

3.4. Porosity

The pore volume results (Table 2) reveal distinct behaviors between tablets produced by BJ and FDM. For both BJ designs, dotted and continuous score lines, the pore volumes are similar (32–36%), regardless of the number of subdivisions. In contrast, FDM tablets exhibited a pronounced reduction in porosity as subdivision complexity increased. For placebo FDM tablets, porosity decreased from 23.86 ± 0.93% for halves to 6.62 ± 1.72% for eighths. A similar trend was observed for drug-loaded FDM tablets, in which porosity decreased from 28.44 ± 0.73% for halves to 5.22 ± 0.39% for eighths.

This difference stems from the fundamental consolidation mechanisms of each process. BJ creates a porous microstructure by selectively depositing binder over a powder bed, joining particles primarily at contact points while retaining interparticle voids [34,39]. Although the binder homogenizes porosity across the structure, minor variations can arise from binder distribution and local geometry [27]. The introduction of dotted scores did not markedly alter the overall pore volume in BJ tablets, but a slight tendency toward increased porosity was observed. This effect could be associated with reduced local densification in the modified score regions, which were purposefully designed to facilitate fracture.

In contrast, FDM printing forms compact, layered structures by depositing and fusing molten polymer filaments [40]. As the number of score lines increases, the model introduces additional perimeter layers surrounding each subdivided section, with more outer shells. These solid boundaries occupy a greater fraction of the total volume, while the infill region between them becomes proportionally smaller. Consequently, the internal void fraction decreases, producing denser tablets with fewer interlayer gaps. This phenomenon explains the strong inverse correlation between subdivision and porosity observed for FDM tablets.

A slightly higher pore volume was observed for the drug-loaded FDM tablets compared with the placebo, particularly for the half and quarter configurations (Table 2). This difference may be attributed to the

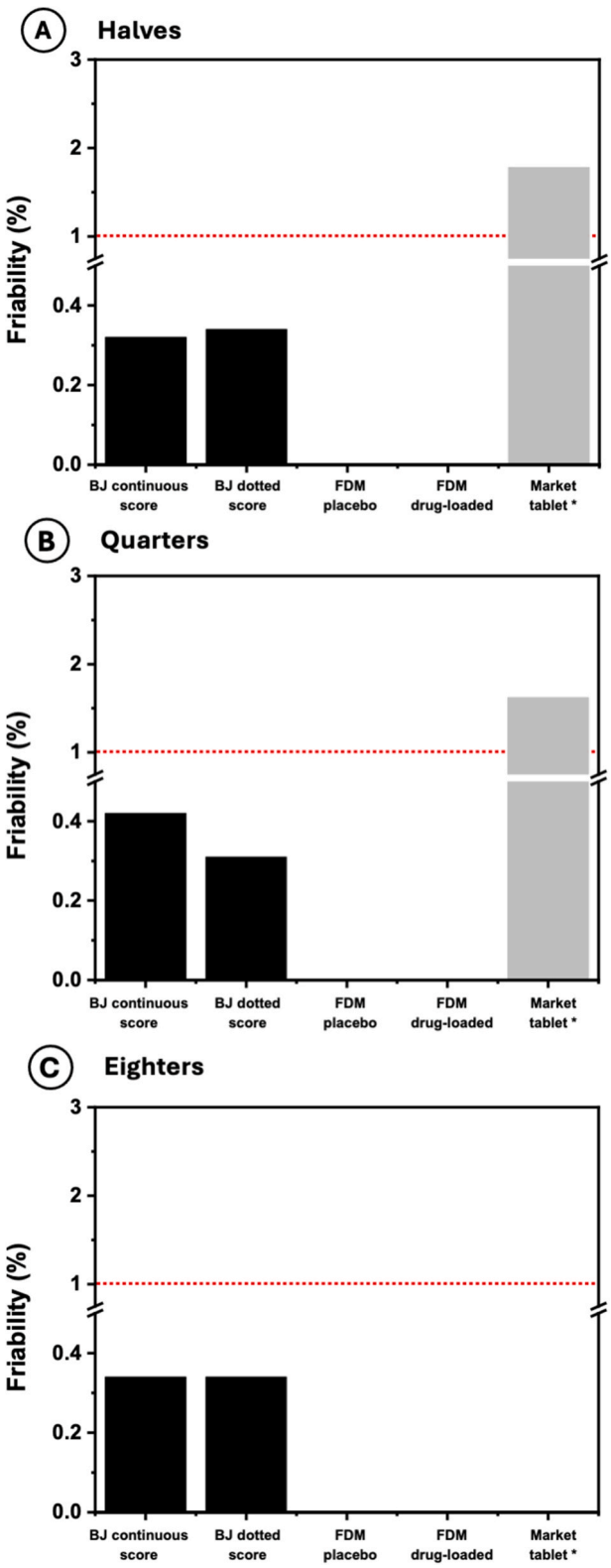

Fig. 6. Friability (%) of detachable 3D-printed tablets fabricated by binder jetting (BJ)—with continuous or dotted score designs—and fused deposition modeling (FDM) —placebo or drug-loaded. Tablets were manually divided into (A) halves, (B) quarters, and (C) eighths. Comparative data for commercial tablets were obtained from the literature ($^{\#}$ [3]; $^{\#\#}$ [35]. ϕ = no data available. The dashed line indicates the FDA guidelines' limits for tablet splitting. * ($p < 0.05$), ** ($p < 0.005$).

Table 2
Pore volume of tablets according to printing technique and number of subdivisions.

Number of subdivisions	Pore volume (%)			
	BJ dotted scores tablets	BJ continuous score tablets	FDM placebo	FDM drug-loaded
2	34.89 ± 0.72^{ab}	32.75 ± 0.61^{b}	23.86 ± 0.93^{c}	28.44 ± 0.73^{f}
4	36.61 ± 0.34^{a}	33.34 ± 1.69^{b}	11.52 ± 0.60^{d}	18.62 ± 0.88^{g}
8	36.67 ± 0.42^{a}	34.88 ± 0.93^{ab}	6.62 ± 1.72^{e}	5.22 ± 0.39^{e}

Different superscript letters (a–g) indicate statistically significant differences ($p < 0.05$) according to Tukey's post-hoc test.

presence of the drug which can modify the rheological behavior of the molten filament during extrusion and deposition. The incorporation of caffeine may reduce melt viscosity and alter the flow and spreading behavior of the deposited strands, leading to less efficient interlayer fusion [41]. In addition, the presence of dispersed drug domains within the polymer matrix may locally interfere with polymer chain interdiffusion during filament welding, further contributing to slightly increased porosity.

Overall, FDM tablets were substantially less porous than BJ-produced tablets, even before subdivision. While BJ inherently produces open-porous matrices due to its particle-binder bonding mechanism, FDM enables tunable compactness through geometric parameters, such as wall count and infill density. This structural distinction is consistent with prior reports showing that BJ parts typically exhibit high porosity and low mechanical strength, whereas FDM products are denser and more mechanically robust [34,40].

3.5. Microscopy

Optical microscopy (Fig. 7) enabled a detailed assessment of the surface topography and feature definition of tablets fabricated by BJ and FDM, with emphasis on the engineered score lines for subdivision into halves, quarters, and eighths.

3D tablets produced by the BJ model with continuous scores exhibited lower-resolution section areas and irregular edges, particularly in tablets intended for multiple subdivisions. In these cases, excess deposited material along the intended fracture lines was evident, which may have contributed to the higher mass loss and mass variation recorded experimentally.

In contrast, BJ dotted-score 3D tablets showed sharper and more well-defined fracture lines, regardless of the number of subdivisions. The dotted pattern appeared to act as a more efficient mechanical guide for crack initiation and propagation, enabling more accurate splitting and reducing mass loss (Fig. 7). This effect was reflected in lower values of mass loss, mass variation, and friability, particularly for tablets divided into quarters and eighths. The dotted-score feature proved especially advantageous as the subdivision complexity increased, becoming critical for successful splitting into eight parts.

FDM 3D tablets (placebo or drug-loaded), on the other hand, exhibited highly regular score lines with superior resolution, characterized by deeper and more uniform contours. The controlled deposition of polymer filaments during layer-by-layer construction resulted in consistent, reproducible score lines. This continuous filament arrangement facilitated directed crack propagation, which was consistent with the low mass variation and negligible mass loss observed across all subdivision conditions.

Differences in printing resolution and edge fidelity were evident between the platforms. In BJ, feature resolution is constrained by powder particle size distribution, layer thickness, and binder droplet dynamics [27,34]. By contrast, FDM constructs the score as a continuous extrudate track with controllable nozzle diameter, road width, and layer height, which tends to yield sharper score line contours and higher geometric fidelity at the score edges compared with powder-bed BJ [42]. FDM typically delivers cleaner, better-defined score morphology due to the absence of powder rearrangement and binder migration at the feature boundary [27,42].

Mechanistically, binder saturation and particle packing in BJ govern neck growth and feature sharpness, whereas in FDM, filament lay down and raster orientation control the local anisotropy at the score root—two levers that rationalize the sharper, more uniform score profiles observed here for FDM and the improved BJ outcomes when the score geometry is optimized (e.g., dotted-score) and binder/post-processing are tuned [34,42].

Overall, despite the inherent limitations of the BJ technique, the findings demonstrate that promising subdivision performance can be achieved through appropriate optimization of tablet geometry. In particular, the adoption of the dotted-score design represents an effective strategy to improve tablet divisibility and ensure dose accuracy in 3D-printed dosage forms manufactured by BJ.

Rather than replacing individualized dose printing, detachable 3D-printed tablets are proposed as a complementary strategy that expands dose-adjustment flexibility in both large-scale and point-of-care 3D-printing settings. This approach provides an intermediate layer of adaptability for scenarios in which rapid or temporary dose adjustments are clinically required or where batch-based 3D printing is adopted at industrial scale.

4. Conclusion

This exploratory study demonstrated that FDM and BJ 3D printing technologies are feasible and effective platforms for the production of detachable tablets, offering significant advantages over conventional manufacturing for accurate and reproducible subdivision. FDM consistently delivered superior outcomes in terms of mass variation, mass loss, friability, and score line definition, primarily due to the cohesive nature of plastic matrices and the higher geometric fidelity inherent to extrusion-based printing. Moreover, the inclusion of a representative drug-loaded FDM formulation further confirmed the robustness of the proposed detachable-tablet design, supporting its translational relevance. On the other hand, BJ, although less resolved, proved capable of achieving satisfactory subdivision performance when optimized through dotted-score design and saline post-treatment.

Taken together, these results reinforce the transformative potential of 3D printing for personalized pharmacotherapy, enabling the creation of dosage forms that combine dose flexibility, mechanical robustness, and regulatory compliance with pharmacopeial requirements. This work establishes a proof-of-concept foundation and opens avenues for future research, particularly focusing on drug-loaded formulations, in vitro and in vivo performance, and scale-up to industrial settings. Such developments could accelerate the translation of 3D-printed detachable tablets into clinical practice, contributing to safer and more effective individualized treatments across a wide range of therapeutic areas, particularly in populations where tablet subdivision is routinely required, such as pediatric and geriatric patients.

Declaration of generative AI and AI-assisted technologies in the writing process

During the preparation of this work, the authors used ChatGPT 4 in order to review the English translation. After using this tool, the authors reviewed and edited the content as needed and took full responsibility for the content of the publication.

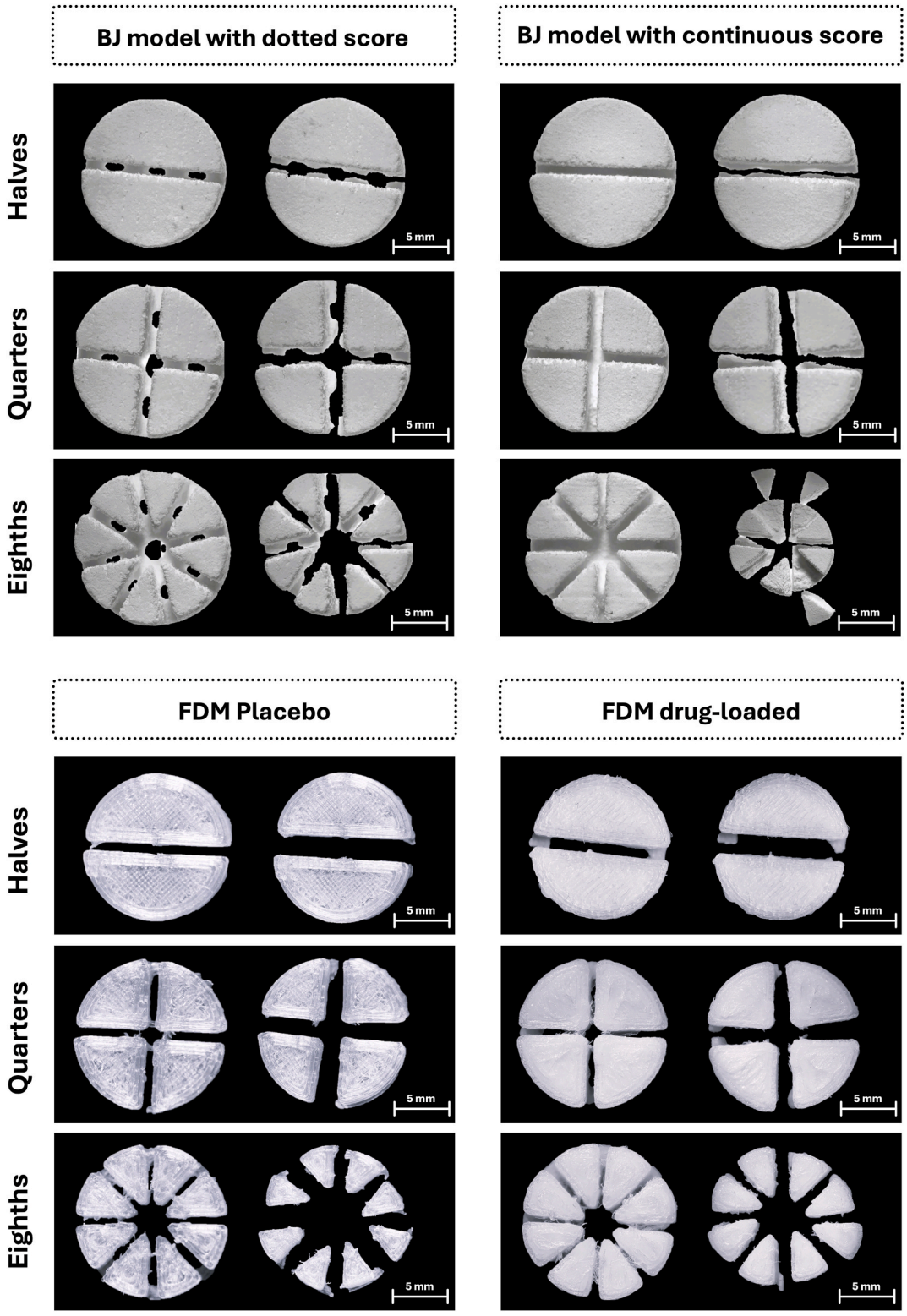

Fig. 7. Optical microscopy images of detachable 3D-printed tablets fabricated by binder jetting (BJ)—with continuous or dotted score designs—and fused deposition modeling (FDM) —placebo or drug-loaded. Tablets were designed to be subdivided into halves, quarters, and eighths. Scale bars represent 5 mm.

CRediT authorship contribution statement

Gabriel S. Oliveira: Formal analysis, Investigation, Methodology, Writing – original draft. **Ana Luiza Lima:** Investigation, Methodology, Visualization. **Idejan P. Gross:** Formal analysis, Methodology, Writing – review & editing. **Ludmila Alvim Gomes Pinho:** Conceptualization, Investigation, Methodology. **Livia Sa-Barreto:** Conceptualization, Funding acquisition, Supervision. **Patrícia Medeiros-Souza:** Funding acquisition, Writing – review & editing. **Tais Gratieri:** Funding acquisition, Writing – review & editing. **Guilherme M. Gelfuso:** Methodology, Writing – review & editing. **Marcilio Cunha-Filho:** Conceptualization, Funding acquisition, Supervision, Writing – review

& editing.

Declaration of competing interest

The authors declare that they have no known competing financial interests or personal relationships that could have appeared to influence the work reported in this paper.

Acknowledgments

The authors gratefully acknowledge the support provided by the University of Brasília (UnB) and the funding agencies Research Support Foundation of the Federal District – FAPDF (Grant n° 527/2024 SEI 00193-00001913/2024-72), CNPq (National Council for Scientific and Technological Development), CAPES (Coordination for the Improvement of Higher Education Personnel), and FINEP (Grant n° 0102/21). Authors also thank Laboratório de Microscopia e Microanálise from the Universidade de Brasilia for microscopy analyses.

Data availability

Data will be made available on request.

References

[1] R. Quinzler, C. Gasse, A. Schneider, P. Kaufmann-Kolle, J. Szecsenyi, W.E. Haefeli, The frequency of inappropriate tablet splitting in primary care, Eur. J. Clin. Pharmacol. 62 (2006) 1065–1073, https://doi.org/10.1007/s00228-006-0202-3.

[2] D.A. van Riet-Nales, M.E. Doeve, A.E. Nicia, S. Teerenstra, K. Notenboom, Y. A. Hekster, et al., The accuracy, precision and sustainability of different techniques for tablet subdivision: breaking by hand and the use of tablet splitters or a kitchen knife, Int. J. Pharm. 466 (2014) 44–51, https://doi.org/10.1016/j.ijpharm.2014.02.031.

[3] M.T. Teixeira, L.C.L. Sá-Barreto, T. Gratieri, G.M. Gelfuso, I.C.R. Silva, M.S. S. Cunha-Filho, Key technical aspects influencing the accuracy of tablet subdivision, AAPS PharmSciTech 18 (2017) 1393–1401, https://doi.org/10.1208/s12249-016-0615-y.

[4] R.B. Shah, J.S. Collier, V.A. Sayeed, A. Bryant, M.J. Habib, M.A. Khan, Tablet splitting of a narrow therapeutic index drug: a case with levothyroxine sodium, AAPS PharmSciTech 11 (2010) 1359–1367, https://doi.org/10.1208/s12249-010-9515-8.

[5] G.S. Oliveira, A.L. Lima, I.P. Gross, L. Sa-Barreto, P. Medeiros-Souza, T. Gratieri, et al., Chromatographic method for determining 6-Mercaptopurine in skin permeation assays for assessing cutaneous exposure risk, ACS Omega 10 (2025) 32384–32390, https://doi.org/10.1021/acsomega.5c04686.

[6] M.T. Teixeira, L.C.L. Sá-Barreto, D.L.M. Silva, M.S.S. Cunha-Filho, Panorama dos aspectos regulatórios que norteiam a partição de comprimidos, Ver. Panam. Salud Publica 39 (2016) 372–377.

[7] D. van Riet–Nales, L. Donkerbroek, A. Nicia, C. Oussoren, A. de Boer, B. van den Bemt, The development of a test battery to assess the hand–eye functions relevant in predicting easy and accurate tablet subdivision in older people: a pilot study, Br. J. Clin. Pharmacol. 86 (2020) 1969–1981, https://doi.org/10.1111/bcp.14201.

[8] H.K. Batchelor, J.F. Marriott, Formulations for children: problems and solutions, Br. J. Clin. Pharmacol. 79 (2015) 405–418, https://doi.org/10.1111/bcp.12268.

[9] N. Drumond, S. Stegemann, Better medicines for older patients: considerations between patient characteristics and solid oral dosage form designs to improve swallowing experience, Pharmaceutics 13 (2021), https://doi.org/10.3390/pharmaceutics13010032.

[10] S. Wilczyński, R. Koprowski, P. Duda, A. Banyś, B. Błońska-Fajfrowska, Microtomographic studies of subdivision of modified-release tablets, Int. J. Pharm. 511 (2016) 899–912, https://doi.org/10.1016/j.ijpharm.2016.07.069.

[11] G.R.S. Pereira, S.F. Taveira, M. Cunha-Filho, R.N. Marreto, The effects of fillers and binders on the accuracy of tablet subdivision, AAPS PharmSciTech 19 (2018) 2929–2933, https://doi.org/10.1208/s12249-018-1144-7.

[12] V.Y. Reddy, M.P. Venkatesh, T.M.P. Kumar, Tablet scoring and its regulatory perspective, Appl. Clin. Res. Clin. Trials Regul. Aff. 1 (2014) 107–110, https://doi.org/10.2174/2213476X01666141107192108.

[13] W.A. Habib, A.S. Alanizi, M.M. Abdelhamid, F.K. Alanizi, Accuracy of tablet splitting: Comparison study between hand splitting and tablet cutter, Saudi Pharm. J. 22 (2014) 454–459, https://doi.org/10.1016/j.jsps.2013.12.014.

[14] T. Sovány, P. Kása, K. Pintye-Hódi, Modeling of subdivision of scored tablets with the application of artificial neural networks, J. Pharm. Sci. 99 (2010) 905–915, https://doi.org/10.1002/jps.21853.

[15] M. Cunha-Filho, M.G. Guilherme, T. Gratieri, Subdivision of modified-release tablets: state-of-the-art and future perspectives, Ther. Deliv. 11 (2020) 285–287, https://doi.org/10.4155/tde-2020-0006.

[16] A. Hoeben, E.A.J. Joosten, M.H.J. van den Beuken-van Everdingen, Personalized medicine: recent progress in cancer therapy, Cancers (Basel) 13 (2021), https://doi.org/10.3390/cancers13020242.

[17] M.M. Sanetta, V. der M. Elsabe, The appropriateness and risks of tablet splitting : medifile : clinical review, S. Afr. Pharmaceut. J. 76 (2009) 30–36. https://hdl.handle.net/10520/EJC82230.

[18] V.V. Melo, G.R. Pereira, A.Q. Soares, I.C. Silva, S.F. Taveira, M. Cunha-Filho, et al., Prevalence of tablet splitting in a Brazilian tertiary care hospital, Pharm. Pract. 18 (2020), https://doi.org/10.18549/pharmpract.2020.2.1910.

[19] A.E. Kasahun, A.K. Sendekie, Are pediatrics taking the prescribed tablet dosage form? Practices of off-label tablet modification in pediatric wards: a prospective observational study, Heliyon 9 (2023) e15109, https://doi.org/10.1016/j.heliyon.2023.e15109.

[20] R.P. Nidanapu, S. Rajan, S. Mahadevan, B. Gitanjali, Tablet splitting of antiepileptic drugs in pediatric epilepsy: potential effect on plasma drug concentrations, Pediatr. Drugs 18 (2016) 451–463, https://doi.org/10.1007/s40272-016-0193-1.

[21] A. Emagn Kasahun, N.M. Joseph, A. Belete, Practices of tablet splitting and dose uniformity of fragments at public hospitals in Ethiopia: a cross-sectional study supported by experimental findings, PLoS One 17 (2022) e0279135, https://doi.org/10.1371/journal.pone.0279135.

[22] D.R. Serrano, A. Kara, I. Yuste, F.C. Luciano, B. Ongoren, B.J. Anaya, et al., 3D Printing Technologies in Personalized Medicine, Nanomedicines, and Biopharmaceuticals, 15, Pharmaceutics, 2023, https://doi.org/10.3390/pharmaceutics15020313.

[23] N. Beer, S. Kaae, N. Genina, S.K. Sporrong, T.L. Alves, J. Hoebert, et al., Magistral compounding with 3D printing: a promising way to achieve personalized medicine, Ther. Innov. Regul. Sci. 57 (2023) 26–36, https://doi.org/10.1007/s43441-022-00436-7.

[24] A.L. Lima, I.P. Gross, L.L. de Sá-Barreto, T. Gratieri, G.M. Gelfuso, M. Cunha-Filho, Extrusion-based systems for topical and transdermal drug delivery, Expet Opin. Drug Deliv. 20 (2023) 979–992, https://doi.org/10.1080/17425247.2023.2241362.

[25] M. Cunha-Filho, R.P.A. Maísa, M.G. Guilherme, T. Gratieri, FDM 3D printing of modified drug-delivery systems using hot melt extrusion: a new approach for individualized therapy, Ther. Deliv. 8 (2017) 957–966, https://doi.org/10.4155/tde-2017-0067.

[26] L.A.G. Pinho, A.L. Lima, L.L. Sa-Barreto, T. Gratieri, G.M. Gelfuso, R.N. Marreto, et al., Preformulation studies to guide the production of medicines by fused deposition modeling 3D printing, AAPS PharmSciTech 22 (2021) 263, https://doi.org/10.1208/s12249-021-02114-7.

[27] X. Chen, S. Wang, J. Wu, S. Duan, X. Wang, X. Hong, et al., The application and challenge of binder jet 3D printing technology in pharmaceutical manufacturing, Pharmaceutics 14 (2022), https://doi.org/10.3390/pharmaceutics14122589.

[28] Y. Khadivi, F. Monajjemzadeh, Advancement in the formulation and development of orally disintegrating tablets: innovation, challenges, and future perspective, J. Drug Deliv. Sci. Technol. 108 (2025) 106965, https://doi.org/10.1016/j.jddst.2025.106965.

[29] F.M. Starling, E.F. Camargos, F. Ferreira, M.P.D. Freitas, J.R.S. Costa, P. Medeiros-Souza, Unavailability of appropriate doses and need for tablet splitting of psychotropic drugs by geriatric patients, Geriatrics Gerontol. Aging 13 (2019) 126–132, https://doi.org/10.5327/Z2447-211520191900035.

[30] N. Dumpa, A. Butreddy, H. Wang, N. Komanduri, S. Bandari, M.A. Repka, 3D printing in personalized drug delivery: an overview of hot-melt extrusion-based fused deposition modeling, Int. J. Pharm. 600 (2021) 120501, https://doi.org/10.1016/j.ijpharm.2021.120501.

[31] M. Yazmine, B. Rincon, Design of 3D printed molds for tablet formation, Am. Soc. Eng. Educ. March, 35805 , (2022).

[32] P. Zhang, J. Li, E.A. Ashour, S. Chung, H. Wang, S.K. Vemula, et al., Development of multiple structured extended release tablets via hot melt extrusion and dual-nozzle fused deposition modeling 3D printing, Int. J. Pharm. 653 (2024) 123905, https://doi.org/10.1016/j.ijpharm.2024.123905.

[33] United States Pharmacopeia (USP). General Chapter <1216> Tablet Friability. United States Pharmacopeial Convention, Rockville, MD, USA.

[34] K. Kreft, Z. Lavrič, T. Stanić, P. Perhavec, R. Dreu, Influence of the binder jetting process parameters and binder liquid composition on the relevant attributes of 3D-Printed tablets, Pharmaceutics 14 (2022), https://doi.org/10.3390/pharmaceutics14081568.

[35] G.R. Bedogni, A.L. Lima, I.P. Gross, T. Gratieri, G.M. Gelfuso, M.C. Lamas, et al., 3D printing as a solution for tablet splitting challenges dedicated to the chagas disease treatment, J. Drug Deliv. Sci. Technol. 106 (2025) 106745, https://doi.org/10.1016/j.jddst.2025.106745.

[36] L. Tessmann, P. Medeiros-Souza, J.C.M. Cordoba, N.U.L. Tavares, V.M. Abílio, D. O. de Matos, I.M.Q.S. Magalhães, Partição de comprimidos antineoplásicos utilizados no tratamento de leucemias agudas em crianças e adolescentes, Revista Brasileira de Cancerologia 66 (2) (2020), https://doi.org/10.32635/2176-9745.RBC.2020v66n2.764.

[37] FDA, Guidance for industry—tablet Scoring: Nomenclature, Labeling, and Data for Evaluation, U.S. Food Drug Adm, 2013, 2013.

[38] M. Cunha-Filho, M.T. Teixeira, V. Santos-Rosales, L.L. Sa-Barreto, R.N. Marreto, M. Martin-Pastor, et al., The subdivision behavior of polymeric tablets, Int. J. Pharm. 568 (2019) 118554, https://doi.org/10.1016/j.ijpharm.2019.118554.

[39] W. Du, X. Ren, Z. Pei, C. Ma, Ceramic binder jetting additive manufacturing: a literature review on density, J. Manuf. Sci. Eng. 142 (2020), https://doi.org/10.1115/1.4046248.

[40] D. Karalia, A. Siamidi, V. Karalis, M. Vlachou, 3D-Printed Oral Dosage Forms: Mechanical Properties, Computational Approaches and Applications, 13, Pharmaceutics, 2021, https://doi.org/10.3390/pharmaceutics13091401.
[41] A.L. Lima, F.Q. Pires, L.A. Hilgert, L.L. Sa-Barreto, T. Gratieri, G.M. Gelfuso, M. Cunha-Filho, Oscillatory shear rheology as an in-process control tool for 3D printing medicines production by fused deposition modeling, J. Manuf. Process. 76 (2022) 850–862, https://doi.org/10.1016/j.jmapro.2022.03.001.
[42] M. Alhijjaj, J. Nasereddin, P. Belton, S. Qi, Impact of processing parameters on the quality of pharmaceutical solid dosage forms produced by fused deposition modeling (FDM), Pharmaceutics 11 (2019), https://doi.org/10.3390/pharmaceutics11120633.